Journal of Biomechanics 44, 2706-2711, 2011

# A comparison of Coulomb and pseudo-Coulomb friction implementations: application to the table contact phase of gymnastics vaulting

M.I. Jackson, M.J. Hiley and M.R. Yeadon

School of Sport, Exercise and Health Sciences, Loughborough University, Loughborough , UK.

## Abstract

In the table contact phase of gymnastics vaulting both dynamic and static friction act. The purpose of this study was to develop a method of simulating Coulomb friction that incorporated both dynamic and static phases and to compare the results with those obtained using a pseudo-Coulomb implementation of friction when applied to the table contact phase of gymnastics vaulting. Kinematic data were obtained from an elite level gymnast performing handspring straight somersault vaults using a Vicon optoelectronic motion capture system. An angle-driven computer model of vaulting that simulated the interaction between a seven-segment gymnast and a single-segment vaulting table during the table contact phase of the vault was developed. Both dynamic and static friction were incorporated within the model by switching between two implementations of the tangential frictional force. Two vaulting trials were used to determine the model parameters by using a genetic algorithm to match simulations to recorded performances. A third independent trial was used to evaluate the model and close agreement was found between the simulation and the recorded performance with an overall difference of 13.5%. The two-state simulation model was found to be capable of replicating performance at take-off and also of replicating key contact phase features such as the normal and tangential motion of the hands. The results of the two-state model were compared to those using a pseudo-Coulomb friction implementation within the simulation model. The two-state model achieved similar overall results to those of the pseudo-Coulomb model but obtained solutions more rapidly.

Keywords: computer simulation, friction, stiction, vaulting, gymnastics

## Introduction

In almost all examples of human movement contact with external bodies is involved and frictional forces act. For example when there is contact between a limb and the ground to arrest a fall, the force acting parallel to the ground is friction. Other examples where frictional forces are encountered are activities such as walking, running, jumping, cross-country skiing, tennis and gymnastics in which friction acts both as a driving force and as a retarding force. The motion of interest for this study was gymnastics vaulting, and in particular the table contact phase of the vault, where frictional forces act between the gymnast's hands and the vaulting table.

When two objects come into contact and there is relative motion between them (sliding) the frictional force is known as dynamic friction. On the other hand if the objects are at rest relative to each other, the frictional force is known as static friction, a state often referred to as "stiction". The table contact phase of gymnastics vaulting is a situation in which both sliding and stiction occur (Figure 1).

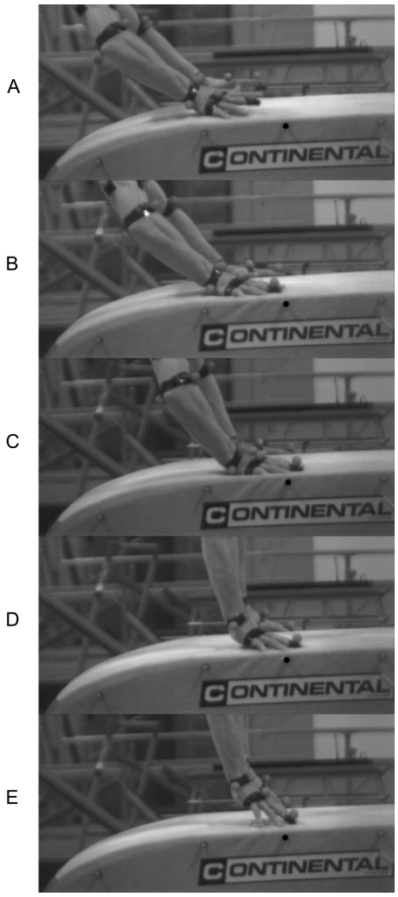


Figure 1. Table contact phase of a handspring entry vault. Note the position of the marker on the finger relative to the position of the marker on the table (indicated in black). A – table contact, B – hands sliding forwards, C – stiction, D – loss of palm contact, E – fingers sliding backwards.

Coulomb's law is commonly used to model frictional forces. During the sliding phase Coulomb's law states that the frictional force $F_{frictional}$ is proportional to the magnitude of the normal contact force $F_{normal}$:

$$\left|F_{frictional}\right| = \mu_k \left|F_{normal}\right| \quad (1)$$

where $\mu_k$ is the coefficient of kinetic friction. During the stiction phase the frictional force is equal in magnitude but opposite in direction to the net force tending to cause motion and hence no motion occurs. In this case Coulomb's law provides a threshold value for the frictional force, above which motion would occur:

$$\left|F_{frictional}\right| \leq \mu_s \left|F_{normal}\right| \quad (2)$$

Application of Coulomb friction switches from stiction to sliding and vice versa. Rather than using two separate computer simulation models to simulate friction in human-ground interactions many researchers have advocated the use of pseudo-Coulomb friction models (McLean et al., 2003; Neptune et al., 2000; Wojtyra, 2003).

A pseudo-Coulomb model is an approximation of Coulomb friction in that instead of having a stationary contact in the stiction phase, sliding continues but with a small velocity. This representation of frictional forces has a number of shortcomings (Bauchau and Ju, 2006). Primarily it alters the physical behaviour of the system as it does not allow stiction to occur and instead systems have the tendency to 'creep'. Furthermore the pseudo-Coulomb representation does not allow for different values of the static and kinetic coefficients of friction. Finally the computation process may be negatively impacted as the relative velocities during the approximated stiction phase may require additional time steps.

To avoid the shortcomings associated with pseudo-Coulomb models, simulation models that transition between stiction and sliding can be used. Imura and Yeadon (2010) developed a simulation model that incorporated both sliding and stiction when representing the frictional forces between the floor and a dancer's foot during a Fouetté turn in ballet. Within Imura and Yeadon's model the dancer was modelled using only two segments which greatly simplified the system and limited the extent to which the model results could be compared to recorded movements. To determine the value of this approach it should be used within a more complex whole body model, and the model results evaluated quantitatively. It may be that such a method provides more accurate or more rapid simulations than a pseudo-Coulomb implementation of friction.

The aim of this study is to implement a method of simulating frictional contacts that incorporates both sliding and stiction and to compare the results with those of a pseudo-Coulomb friction implementation. The two implementations are applied to the table contact phase of gymnastics vaulting and are assessed by comparing simulations to recorded vaulting performances.

## Methods

Subsections in 'Methods' describe the processes used to develop and evaluate a simulation model of gymnastics vaulting. Initially performance data were collected from an elite level gymnast. An angle-driven model of vaulting was developed and angle-driven simulations were matched to the performance data to determine those model parameters that could not be calculated directly. Finally the model was assessed by comparing simulation and performance data of an independent trial with friction implemented as two-state Coulomb friction and single state pseudo-Coulomb friction.

### *Performance Data Collection*

A Vicon optoelectronic motion capture system situated within the National Gymnastics Performance and Research Centre at Loughborough University was used to collect kinematic data of gymnastics vaulting. The participant, an elite male gymnast (21 years, 69.9 kg, 1.73 m), gave informed consent to perform six straight handspring somersault vaults (Figure 2). An international Brevet judge assessed and ranked the performance of each vault, with the best three vaults selected for subsequent analysis.

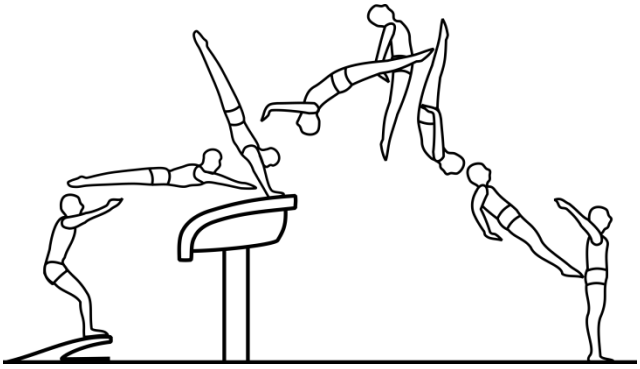

Figure 2. Handspring straight somersault vault (adapted from the FIG Code of Points, 2009).

18 Vicon cameras, sampling at a frequency of 480 Hz, were used to track the motion of markers attached to the gymnast and the vaulting table during the vaulting performances. The cameras were positioned and focused to give a capture volume that encompassed the vaulting board, the vaulting table and the landing mat (10m x 2m x 4m). 58 spherical markers, of 25 mm diameter, were attached to the gymnast. An additional 42 spherical markers, of 15 mm diameter, were attached to the vaulting table and the floor under the vaulting table (Figure 3).

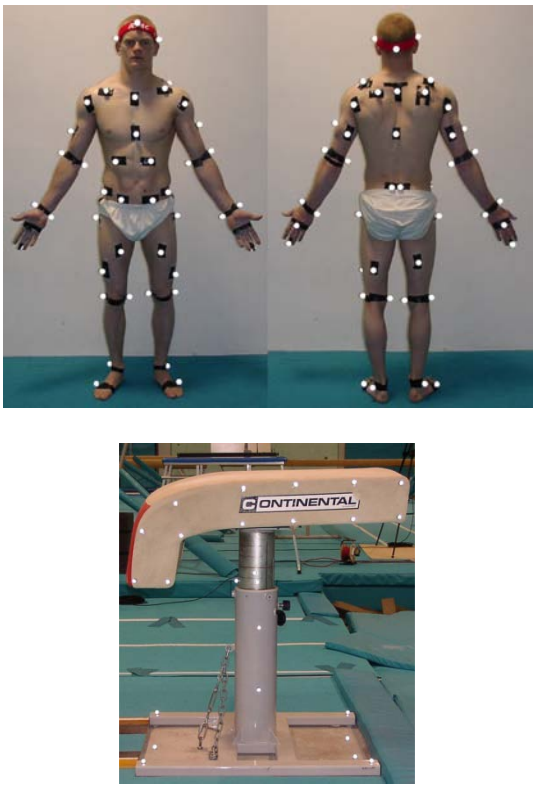


Figure 3. Marker placement on gymnast and vaulting table.

The kinematic data collected using the Vicon motion capture system were processed using a chain model and global optimisation procedure, similar to that used by Begon et al. (2008), to determine the motion of both the gymnast and the table during the table contact phase of each vaulting trial. The large number of markers used within the data collection provided some redundancy which the chain model accommodated. The three-dimensional gymnast chain model comprised 12 segments corresponding to head + upper trunk, lower trunk and left and right thighs, shanks, arms, palms and fingers, while the table was also included as a single segment. Within the model the motions of the left and right limbs were assumed to be symmetrical while upper trunk movement was expressed as a function of hip angle as in Yeadon (1990b) and gleno-humeral joint centre movement was a function of shoulder angle similar to Begon et al. (2008) and Hiley et al. (2009). Shoulder protraction/retraction was included by effectively allowing the arm length to change.

Upper trunk orientation was determined along with hip angle, knee angle, shoulder angle, wrist angle, knuckle angle, the amount of shoulder retraction/protraction and table position and orientation by minimising the distances between the chain model determined marker coordinates and the recorded marker coordinates. The processed kinematic data were fitted using quintic splines (Wood and Jennings, 1979) in order that derivatives and interpolated values could be obtained.

Ninety-five anthropometric measurements were taken from the gymnast and gymnast-specific segmental inertia parameters were calculated using the model of Yeadon (1990a). The gymnast's centre of mass position was determined from the kinematic data using the segmental inertia parameters. The mass and linear dimensions of the vaulting table were measured and the inertial parameters calculated by approximating the table-top and base-frame using a number of cylindrical and cuboidal elements.

A high speed camera sampling at a frequency of 960 Hz was positioned perpendicular to the vaulting runway to capture hand contact with the vaulting table. The camera was triggered such that hand contact occurred approximately in the middle of the video data capture.

### *Simulation Model Development*

A two-dimensional angle-driven simulation model of gymnastics vaulting was developed using the simulation software package Autolev$^{TM}$. The model simulated the interaction between the gymnast and the vaulting table during the table contact phase of the vault. The model described here is a kinematically driven model which allows the calculation of system parameters together with an assessment of model accuracy so that the two friction implementations can be compared. A torque-driven version of the model would enable hypothetical questions to be answered such as optimum technique during table contact for maximising height in post-flight.

The gymnast was modelled using a seven segment model which was equivalent to the 12 segment three-dimensional chain model but made planar by using segments which represented the combined left and right limbs. As such the seven segments corresponded to the head + upper trunk, lower trunk, thighs, shanks, arms, palms and fingers, with each segment having mass, length and moment of inertia such that they represented the body segments of the gymnast. A damped linear spring was used to represent the shoulder retraction and protraction whilst a damped torsional spring was used to represent flexion/extension of the

fingers. Displacement of the glenohumeral joint centre and flexion/extension of the trunk were modelled as functions of shoulder and hip angle respectively as in the chain model (Figure 4).

The table was modelled as a single rigid body with mass, dimensions and moment of inertia such that it was representative of the vaulting table. The contact surface, which was represented by a plane, was defined relative to the table, based on the position that the gymnast initially contacted the vaulting table (Figure 4). A non-linear damped torsional spring allowed the table to rotate about the centre of rotation which was determined from the movement of the table markers.

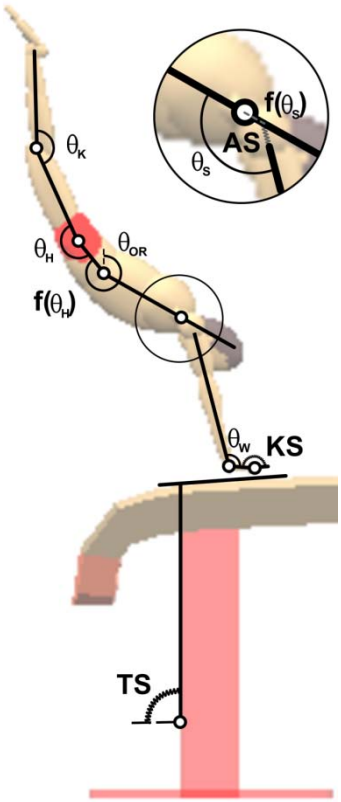


Figure 4. Vaulting table contact phase simulation model. Angles: $\theta_{OR}$ orientation angle, $\theta_W$ wrist angle, $\theta_S$ shoulder angle, $\theta_H$ hip angle, $\theta_K$ knee angle. Constraints: $f(\theta_H)$ lower trunk angle, $f(\theta_S)$ glenohumeral joint centre position. Parameters: AS arm spring, TS table spring, KS knuckle spring.

The interaction between the gymnast and the table was modelled by considering the components of the reaction force normal and tangential to the table surface. In the normal direction the high speed video indicated that the gymnast's hands deformed the surface of the vaulting table. To model the motion of the hands and compression of the table, the normal contact force $R_{ni}$ was represented by spring-dampers situated at three points of contact: the fingertip, the knuckle and the base of the palm:

$$R_{ni} = -K_{CS} d_i - D_{CS} v_i \left| d_i \right| \quad (\textit{for } i = 1,2,3) \tag{3}$$

where $d_i$ and $v_i$ are the displacement and velocity in the direction normal to the contact surface, $K_{CS}$ and $D_{CS}$ are the stiffness and damping coefficients of the table

surface and *i* represents the three points of contact on the hand. Since the gymnast's hands approached the table with a non-zero velocity the damping term was a function of the displacement of the hands to avoid force discontinuities.

In the tangential direction the high speed video indicated that when the gymnast contacted the vaulting table the hands initially slid tangentially along the surface, paused in a stationary position and then slid again before take-off. To model the motion of the hands, allowing for both sliding and stiction, a two-state tangential contact force implementation was used. Two separate simulation models were generated using Autolev$^{TM}$, each of which was governed by a different set of equations of motion. Within the sliding phase model the tangential frictional force $R_{ti}$ was modelled as dynamic friction:

$$\left|R_{ti}\right| = \mu_k \left|R_{ni}\right| \quad (\textit{for } i = 1,2,3) \tag{4}$$

where $\mu_k$ is the coefficient of kinetic friction. The tangential frictional force acted in the opposite direction to the tangential velocity of the hands. Within the stiction phase model the degree of freedom in the tangential direction was removed, constraining the tangential hand velocity to zero. The force required to keep the hands stationary (the stiction frictional force) was determined with equation (2) to identify the transition from stiction to sliding.

The sliding phase and stiction phase models were used sequentially to represent the tangential contact force during the table contact phase. When the gymnast came into contact with the table the sliding phase began. When the tangential velocity dropped below $v_0 = 0.01$ ms$^{-1}$ the implementation switched to the stiction phase (zero tangential velocity). While the stiction frictional force was less than the limiting frictional force, the stiction phase continued. When the stiction frictional force became greater than limiting friction, the implementation switched back to the sliding phase model and the hands slid again.

A pseudo-Coulomb simulation model, similar to that used by McLean et al. (2003) was also implemented. This model only differed from the two-state simulation model in the implementation of the tangential contact force, where the force was modelled as an approximation of Coulomb friction:

$$\left|R_{ti}\right| = \mu \left|R_{ni}\right| \quad (\textit{for } i = 1,2,3) \quad \text{if } \left|v_{fin}\right| > v_{\lim}$$

$$\left|R_{ti}\right| = -bv_i \quad (\textit{for } i = 1,2,3) \quad \text{if } \left|v_{fin}\right| < v_{\lim} \tag{5}$$

where *b* is a large positive constant and $v_{lim}$ is a constant velocity limit.

### *Model Parameter Determination*

The two-state simulation model was driven with joint angle time histories obtained from the recorded performances to determine the model parameters which could not be calculated directly. These included the viscoelastic parameters of the shoulder, knuckle, table and contact springs and the static and kinetic coefficients of friction between the hands and the contact surface. These model parameters were determined by matching simulations to recorded performances.

The initial conditions just prior to contact with the vaulting table (position and velocity of the gymnast's centre of mass and orientation and angular velocity of the upper trunk segment) were taken from the recorded performances and input to the model. The model was driven with joint angle time histories of the shoulder, wrist, hip and knee from the recorded performances. The output from the model included: the gymnast's centre of mass position and velocity at take-off, the orientation and angular velocity of the gymnast's trunk at take-off, and the orientation of the table at take-off.

A genetic algorithm (Carroll, 2001) was employed to minimise an objective difference score in order to match simulations with recorded performances by varying the model parameters. The objective difference score measured the difference between a simulation and performance using four performance components ($P_i$), and five system components ($S_i$). The $P_i$ defined the takeoff conditions which are crucial for any simulation study of performance while the $S_i$ included measures that would enable the determination of system parameters such as the viscoelastic parameters of the shoulder, knuckle, table and contact springs and the coefficient of friction between the hands and the contact surface. The components comprised: $P_1$ - difference in upper trunk orientation at take-off in degrees, $P_2$ - % difference in angular velocity at take-off, $P_3$ - % difference in horizontal linear velocity at take-off, $P_4$ - % difference in vertical linear velocity at take-off, $S_1$ - Root mean square (RMS) difference in the displacement of the shoulders (shoulder retraction and protraction) during contact as a percentage of the maximum displacement of the shoulders during contact, $S_2$ - RMS difference in the angular displacement of the table during contact as a percentage of the maximum angular displacement of the table during contact, $S_3$ - Average % difference in maximum normal depression of the three contact points during contact, $S_4$ - % difference in maximum tangential displacement of the fingertip during contact, $S_5$ - % difference in contact time. The overall score was calculated by taking a weighted RMS of the nine components. The performance and system categories were each given a 50% weighting and within each category the components were equally weighted, where 1° was considered comparable to a 1% difference in other measures:

$$Score = \sqrt{\left(\frac{P_1^{\,2} + P_2^{\,2} + P_3^{\,2} + P_4^{\,2}}{8}\right) + \left(\frac{S_1^{\,2} + S_2^{\,2} + S_3^{\,2} + S_4^{\,2} + S_5^{\,2}}{10}\right)} \qquad (6)$$

In order to obtain a robust set of parameters that may be used generally for similar movements, Wilson et al. (2006) found that more than one performance should be used when determining parameters. Hence, two vaulting performances, $L_1$ (judged best performance) and $L_2$ (judged third best performance) were used to determine the model parameters. Each vault was first matched individually to obtain an initial estimate of the parameter values and then the two vaults were matched concurrently, by minimising the mean of the two difference scores, to determine the final common set of parameter values. The genetic optimisation algorithm was run for a fixed number of generations (200) and then a check for convergence was made.

The model parameter determination process described above was repeated for the pseudo-Coulomb model to find the parameters for this model including $b$ and $v_{lim}$.

### *Assessment*

To assess the performance of the Coulomb and pseudo-Coulomb implementations of the vaulting model using their respective parameter sets from the combined matching, an independent trial $L_3$ (second best performance) was used to compare simulations with the recorded performance.

## Results

The optimised model parameters of the two-state model (Table 1) lead to overall difference scores of 12.9% (3.9% performance and 17.9% system) for $L_1$ and 11.6% (3.8% performance and 16.0% system) for $L_2$. When the two-state model was evaluated using the independent vault ($L_3$) similar agreement was found between simulation and performance with an overall score of 13.5% (3.4% performance and 18.8% system). Visual representations of the table contact phase during the recorded performance and the simulation of vault $L_3$ show close agreement (Figure 5).

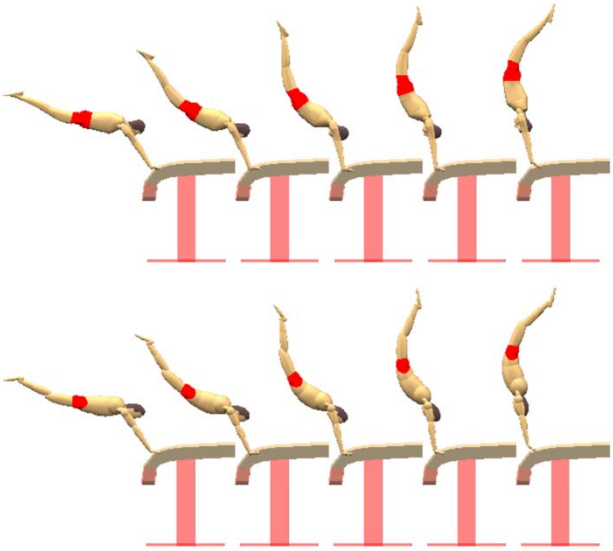

Figure 5. Graphics sequences of table contact phase of vault $L_3$: performance (upper) and two-state model angle-driven simulation (lower).

When vault $L_3$ was simulated using the pseudo-Coulomb model parameters (Table 2) the overall score was 14.1% (3.9% performance and 19.5% system). While this is comparable to that obtained using the two-state model (13.5%) the simulation took considerably longer to run (820 ms compared to 240 ms when using the two-state model). The parameters for the pseudo-Coulomb model were similar to those of the two-state model (Table 2, Table 1) as were the individual performance and system difference scores (Table 3).

Table 1. Two-state model parameters determined from combined matching

| Parameter | | |
|---|---|---|
| Table contact stiffness ($K_{CS}$) | (N $m^{-1}$) | 153000 |
| Table contact damping ($D_{CS}$) | (Ns $m^{-2}$) | 298 |
| Knuckle torsional stiffness ($K_{KT}$) | (Nm $rad^{-1}$) | 228 |
| Knuckle torsional damping ($D_{KT}$) | (Nms $rad^{-1}$) | 5.65 |
| Shoulder stiffness ($K_{SH}$) | (N $m^{-1}$) | 11300 |
| Shoulder damping ($D_{SH}$) | (Ns $m^{-1}$) | 513 |
| Table torsional stiffness 1 ($K_{TT1}$) | (Nm $rad^{-1}$) | 145000 |
| Table torsional stiffness 2 ($K_{TT2}$) | (Nm $rad^{-2}$) | 21100000 |
| Table torsional damping ($D_{TT}$) | (Nms $rad^{-2}$) | 108 |
| Coefficient of kinetic friction ($\mu_k$) | | 0.732 |
| Coefficient of static friction ($\mu_s$) | | 0.775 |
| Limiting velocity ($v_0$) | (m $s^{-1}$) | 0.01 |

Table 2. Pseudo-Coulomb model parameters determined from combined matching

| Parameter | | |
|---|---|---|
| Table contact stiffness ($K_{CS}$) | (N $m^{-1}$) | 155000 |
| Table contact damping ($D_{CS}$) | (Ns $m^{-2}$) | 248 |
| Knuckle torsional stiffness ($K_{KT}$) | (Nm $rad^{-1}$) | 226 |
| Knuckle torsional damping ($D_{KT}$) | (Nms $rad^{-1}$) | 4.65 |
| Shoulder stiffness ($K_{SH}$) | (N $m^{-1}$) | 11500 |
| Shoulder damping ($D_{SH}$) | (Ns $m^{-1}$) | 366 |
| Table torsional stiffness 1 ($K_{TT1}$) | (Nm $rad^{-1}$) | 116000 |
| Table torsional stiffness 2 ($K_{TT2}$) | (Nm $rad^{-2}$) | 20100000 |
| Table torsional damping ($D_{TT}$) | (Nms $rad^{-2}$) | 211 |
| Coefficient of friction ($\mu$) | | 0.774 |
| Psuedo-Coulomb constant (b) | (kg $s^{-1}$) | 2870 |
| Limiting velocity ($v_{lim}$) | (m $s^{-1}$) | 0.589 |

Table 3. Difference scores for the two models

| | Two-state | | | Pseudo-Coulomb | | |
|---|---|---|---|---|---|---|
| | $L_1$ | $L_2$ | $L_3$ | $L_1$ | $L_2$ | $L_3$ |
| $P_1$ (°) | 0.9 | 1.2 | 0.9 | 1.5 | 1.3 | 1.2 |
| $P_2$ (%) | 5.8 | 5.2 | 5.2 | 4.4 | 4.4 | 3.3 |
| $P_3$ (%) | 5.3 | 0.4 | 2.1 | 6.6 | 2.3 | 4.1 |
| $P_4$ (%) | 0.2 | 5.5 | 3.6 | 2.4 | 7.7 | 5.6 |
| $S_1$ (%) | 14.8 | 8.6 | 14.9 | 9.8 | 9.2 | 11.3 |
| $S_2$ (%) | 12.6 | 10.9 | 17.3 | 12.6 | 12.4 | 20.1 |
| $S_3$ (%) | 34.3 | 30.4 | 32.3 | 32.1 | 32.1 | 32.0 |
| $S_4$ (%) | 3.0 | 11.2 | 13.2 | 3.3 | 1.8 | 17.7 |
| $S_5$ (%) | 5.7 | 5.1 | 5.4 | 5.3 | 4.2 | 5.6 |
| P (%) | 3.9 | 3.8 | 3.4 | 4.2 | 4.6 | 3.9 |
| S (%) | 17.9 | 16.0 | 18.8 | 16.3 | 16.1 | 19.5 |
| Overall (%) | 12.9 | 11.6 | 13.5 | 11.9 | 11.8 | 14.1 |

For both models the simulations resulted in performances in which key contact phase features were similar to those seen in the recorded performances, namely: the movement of the arm replicated the recorded movement with shoulder retraction during the initial part of the contact phase and shoulder protraction during the later part of the contact phase (RMS differences throughout the contact phase of 12 mm (two-state model) and 9 mm (pseudo-Coulomb model) respectively); the fingertip, knuckle and base of the palm all deformed the table in the normal direction; the duration of the table contact was similar to the recorded performance (differences of 9 ms (two-state model) and 10 ms (pseudo-Coulomb model) respectively) and the table oscillated with appropriate amplitude and frequency during the contact phase (Figure 6).

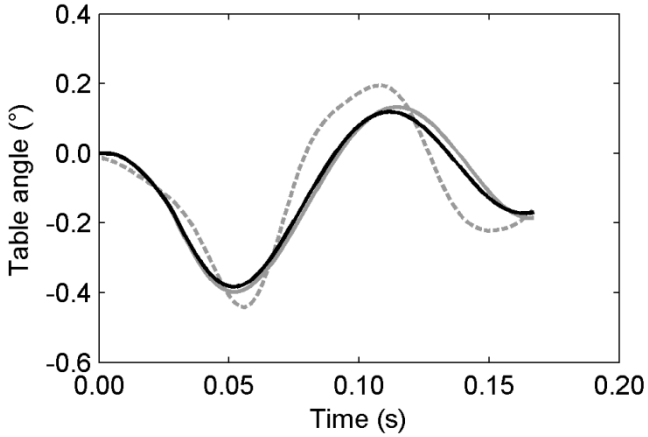


Figure 6. Comparison of table angular displacement during the table contact phase of vault $L_3$: performance (dashed line), two-state model simulation (black line) and pseudo-Coulomb model simulation (grey line).

Although there were qualitative differences in the tangential movement of the hands relative to the table, the difference in hand displacements between the two models of friction were less than 3 mm (Figure 7).

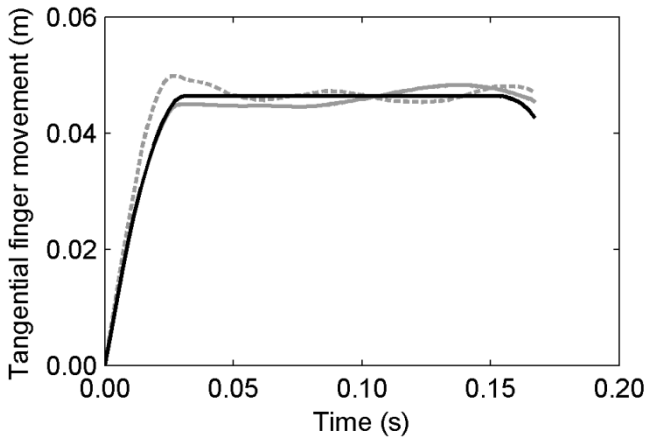


Figure 7. Comparison of tangential finger displacement during the table contact phase of vault $L_3$: performance (dashed line), two-state model simulation (black line) and pseudo-Coulomb model simulation (grey line).

## Discussion

A simulation model of gymnastics vaulting that incorporated both dynamic and static friction was implemented. The simulation model and model parameters were successfully evaluated, with close agreement found between recorded performance and simulation. The performance difference scores were low at 3-4% but the system difference scores had larger values of 16-20%. The system difference scores may have been high due to the difficulty in obtaining accurate measurements of hand displacement, shoulder displacement, table rotation and table depression together with the relatively small amplitudes of these measures. However the simulation model was found to be capable of not only replicating performance at take-off but also of replicating key contact phase features. This indicates that the simulation model and the combined matching parameter set can be used generally for handspring straight somersault vaults.

The two-state tangential contact force implementation allowed for stiction during the table contact phase, and was thus a more correct representation of Coulomb friction than the pseudo-Coulomb model in which the hands 'crept' during the table contact phase. The two-state model allowed different coefficients of friction for the stiction and and sliding phases whereas the pseudo-Coulomb model did not. Both representations, however, gave hand displacements close to those obtained from the motion capture values. In this application the static and kinetic coefficients of friction were similar (0.73 and 0.78, Table 1) but could be markedly different in other applications. The two-state tangential contact force implementation introduces discontinuities at the switchover points between sliding and stiction but these do not cause integration problems since simulations are stopped and then restarted.

An advantage of the two-state model was that simulations ran more than three times faster than the pseudo-Coulomb model. Within the pseudo-Coulomb model the hands continue to move with a small velocity relative to the table when in reality there is no relative motion and these small velocities require the integration algorithm to use a reduced step size, slowing the solution evaluation. The shorter run time for the two-state model is likely to be of considerable advantage in optimisation studies in which hundreds of thousands of simulations are run. In the current application to gymnastics vaulting an optimisation of contact technique using a torque driven model to produce maximum rotation, for example, could involve more than 200,000 individual simulations with a run time of the order of two days. In such circumstances whether an implementation runs three times faster or slower than another can be of considerable importance. A two-state friction implementation should be applied to other situations in which frictional contacts occur and when short computation times are required.

**Acknowledgement**

The support of British Gymnastics is gratefully acknowledged.

**References**

Bauchau, O. and Ju, C. (2006). Modeling frictional phenomena in flexible multibody dynamics. *Computer Methods in Applied Mechanics and Engineering*, 195 (50), 6909-6924.

Begon, M., Wieber, P., and Yeadon, M. (2008). Kinematics estimation of straddled movements on high bar from a limited number of skin markers using a chain model. *Journal of Biomechanics*, 41 (3), 581-586.

Carroll, D. L. (2001). FORTRAN genetic algorithm driver. Downloaded from: http://cuaerospace.com/carroll.ga.html

Fédération Internationale de Gymnastique - FIG (2009). *Code of Points – Men's Technical Committee*. FIG, Switzerland.

Hiley, M., Wangler, R., and Predescu, G. (2009). Optimization of the flege on parallel bars. *Sports Biomechanics*, 8 (1), 39-51.

Imura, A. and Yeadon, M. R. (2010). Mechanics of the Fouetté turn. *Human Movement Science*, 29 (6), 947-955.

McLean, S. G., Su, A., and van den Bogert, A. J. (2003). Development and validation of a 3-D model to predict knee joint loading during dynamic movement. *Journal of Biomechanical Engineering*, 125 (6), 864-874.

Neptune, R., Wrigth, I., and van den Bogert, A. J. (2000). A method for numerical simulation of single limb ground contact events: application to heel-toe running. *Journal of Computer Methods in Biomechanics and Biomedical Engineering*, 3, 321-334.

Wilson, C., King, M., and Yeadon, M. (2006). Determination of subject-specific model parameters for visco-elastic elements. *Journal of Biomechanics*, 39 (10), 1883-1890.

Wojtyra, M. (2003). Multibody simulation model of human walking. *Mechanics Based Design of Structures and Machines*, 31 (3), 357-379.

Wood, G. A. and Jennings, L. S. (1979). On the use of spine functions for data smoothing. *Journal of Biomechanics*, 12 (6), 477-479.

Yeadon, M. R. (1990a). The simulation of aerial movement – II. A mathematical inertia model of the human body. *Journal of Biomechanics*, 23 (1), 67-74.

Yeadon, M. R. (1990b). The simulation of aerial movement – III. The determination of the angular momentum of the human body. *Journal of Biomechanics*, 23 (1), 75-83.